Hindawi Publishing Corporation
International Journal of Rotating Machinery
Volume 2008, Article ID 657202, 10 pages
doi:10.1155/2008/657202

Research Article

Simulation of Casing Treatments of a Transonic Compressor Stage

M. Hembera,[1] H.-P. Kau,[1] and E. Johann[2]

[1] *Institute for Flight Propulsion, Technische Universität München, Boltzmannstraße 15, 85747 Garching, Germany*
[2] *Compressor Aerodynamics, Rolls-Royce Deutschland, Eschenweg 11, 15827 Dahlewitz Berlin, Germany*

Correspondence should be addressed to M. Hembera, hembera@tum.de

Received 31 March 2008; Accepted 1 October 2008

Recommended by Chunill Hah

This article presents the study of casing treatments on an axial compressor stage for improving stability and enhancing stall margin. So far, many simulations of casing treatments on single rotor or rotor-stator configurations were performed. But as the application of casing treatments in engines will be in a multistage compressor, in this study, the axial slots are applied to a typical transonic first stage of a high-pressure 4.5-stage compressor including an upstream IGV, rotor, and stator. The unsteady simulations are performed with a three-dimensional time accurate Favre-averaged Navier-stokes flow solver. In order to resolve all important flow mechanisms appearing through the use of casing treatments, a computational multiblock grid consisting of approximately 2.4 million nodes was used for the simulations. The configurations include axial slots in 4 different variations with an axial extension ranging into the blade passage of the IGV. Their shape is semicircular with no inclination in circumferential direction. The simulations proved the effectiveness of casing treatments with an upstream stator. However, the results also showed that the slots have to be carefully positioned relative to the stator location.

1. INTRODUCTION

In order to reduce weight and enhance efficiency of compressors for modern jet engines, the requirements for the power density are further rising. This is among other things achieved by increasing the rotational speed so that the blade tips of the first rotor stage are operating in transonic conditions. Developments lead to an increase of the aerodynamic loading of the blades, also rise the risk of rotating stall and surge during operations. This risk can be countered through the application of casing treatments.

In the last 40 years, many casing treatments above the rotor have been tested and simulated. It is proven that these devices can extend the stall margin of a compressor. The treatments are only useful when the rotor tip is responsible for stall. The rotor has to be tip-critical.

The casing treatment can be classified into two categories according to their geometric configuration:

(1) circumferential treatments such as circumferential grooves, which are typically axis-symmetric,

(2) axial treatments such as axial slots, which are non-axis-symmetric.

These two categories and the different shapes therein are not equally effective in terms of stall margin enhancement and efficiency loss [1–16]. In general, the most successful treatments in terms of mass flow reduction at stall are axial slots, which are used in this study.

Many studies were conducted to identify and analyze the flow mechanisms in these highly loaded transonic compressor stages at design point and at operation points close to surge, both for design and off-design speeds. The investigations identified two main groups of stall mechanisms: flow instabilities resulting from complex blade tip effects and common blade stall (Greitzer et al. [4]). The latter occurs due to an excessive flow deflection resulting in an increased aerodynamic loading of a compressor blade. This overloading causes the onset of widely spread flow separations at the suction side of the blade hence blocking the passage flow. It was shown that blade stall effects can be delayed successfully through increasing the airfoil's

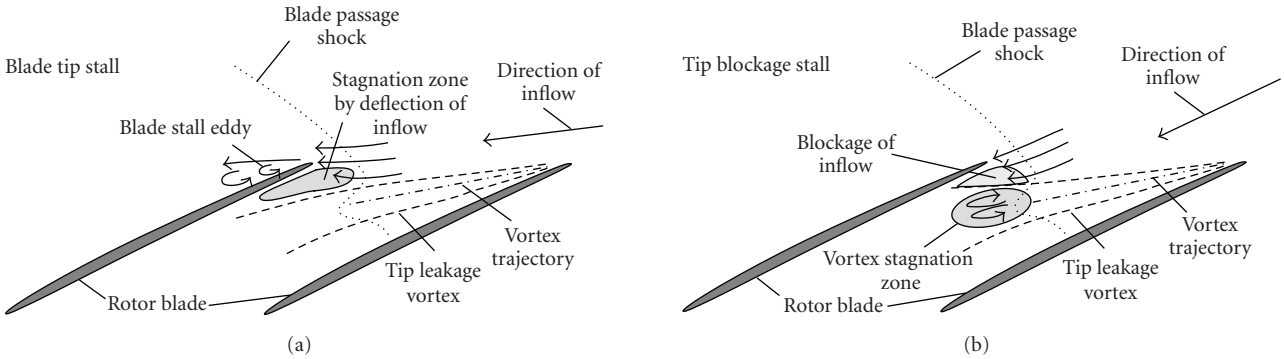

Figure 1: Blade tip stall and tip blockage stall.

solidity. However, compressor stages can also experience stall although the aerodynamic loading of the blades does not exceed a stability limit. Here, complex flow mechanisms, which occur near the blade tip clearance, are found to be the key factor for the limited stability.

Most of the investigated casing treatments in the last decades enhance flow stability, but, unfortunately, also most of them come along with an often significant drop in efficiency. Many investigations were conducted with the goal to understand the specific impact of casing treatments on the compressor flow, but many basic questions still remain unsolved. Until now, for example, it is not yet clear why some casing treatment configurations perform very well in some compressor systems at certain speeds, but fail at other operation speeds or on other compressor systems. No design guidelines, for casing treatments in order to apply a specific geometry of a casing treatment to the individual requirements of a compressor stage, exist so far. The only fact that is proven is that blade tip effects have to be responsible for the onset of stall mechanisms so that the application of casing treatments can successfully enhance the stability of the compressor (Greitzer et al. [4]).

The first part of the following study is dealing with the understanding of stall inception mechanisms in transonic compressor stages. The second part of the study presents the results of axial slots successfully simulated on a transonic rotor-stator configuration (Wilke and Kau [11]) applied on this specific transonic IGV-rotor-stator configuration.

2. CONSIDERATIONS ON DESIGNING A CASING TREATMENT FOR TRANSONIC COMPRESSORS

Casing Treatments for compressors are designed in order to effectively enhance its flow stability under critical flow conditions without dropping the performance of the compressors. This is possible if the casing treatment is able to manipulate the specific flow mechanisms which are responsible for compressor stall and at the same time minimizing unnecessary casing treatment flow in normal compressor operations. The two different phenomena, blade tip stall and tip blockage stall were identified as the two basic mechanisms of tip stall in transonic compressors in detailed simulations conducted in previous investigations with different transonic compressors. Both stall classes can occur in combination or as isolated phenomena depending on the aerodynamic design. This fact is one of the explanations why the impact of casing treatments can change significantly with the speed of rotation or the type of compressor.

2.1. Blade tip stall

At blade tip stall, the angle of attack of the inflow is very steep especially near the blade tip. Thus, the inflow cannot completely follow the direction given by the blade profile. This results in an extended separation zone at the blade suction side and a significant deceleration or even stagnation of the inflow at the upstream part of the following blade pressure side (see Figure 1). The tip leakage flow and the tip leakage vortex rather just fill up the separation zone at the suction side of the blade than blocking the incoming flow. The trajectory of the tip leakage vortex is almost parallel to the direction of the inflow.

2.2. Tip blockage stall

At tip blockage stall conditions, the inflow direction of the compressor's main flow is very similar to that of the design point, even close to surge. The angle of attack corresponds with the stagger angle of the rotor blades and the deflection of the flow over the blade passage is moderate. No aerodynamic overloading of the blade tip occurs at the tip blockage stall mechanism. However, at higher pressure loads, the tip leakage flow and the tip leakage vortex can cause a characteristic stagnation zone at the blade passage shock, which leads to a critical blockage of the main flow. The stagnation zone can be the result of a vortex breakdown occurring after the blade passage shock. The angle between the vortex trajectory and the blade chord is significantly bigger than that between the inflow and the blade chord (see Figure 1).

In contrast to blade tip stall, the tip blockage stall mechanism is in general characteristic for high rotational speeds as the phenomenon seems to be a characteristic property of transonic compressors (Wilke et al. [11, 12], Hofmann and Ballmann [17, 18], Schlechtriem and Lötzerich [19], Furukawa et al. [20], Hoeger et al. [21]).

The strategies in designing a casing treatment must be to prevent or to reduce any blockage and stagnation zones induced by the tip leakage flow. Additionally, the inflow near the outer casing should be deflected in the direction of the blade chord in order to avoid an aerodynamic overloading of the blades. Minimizing the tip leakage flow induced stagnation or blockage zones can be achieved through three different arrangements:

(1) reduction of the tip leakage flow, for example, by reducing the blade tip gap;

(2) removing of stagnating leakage flow, for example, by axial slots (Wilke and Kau [22]);

(3) deflection of the flow direction of the tip leakage parallel to the main flow, for example, by circumferential grooves (Wilke and Kau [23]).

A decrease of the inflow angle of attack near the blade tip requires a significant increase of the local mass flow which can be achieved by bleeding additional air out of the blade passage and reinjecting it upstream into the blade passage.

Tip blockage stall effects occur at higher mass flows than blade tip stall mechanisms. Hence, in compressors, in which the flow stability is limited by tip blockage stall effects, the application of casing treatments is generally more effective than in those that show mainly blade tip stall mechanisms. A compressor that experiences tip blockage stall can be stabilized by treating the tip leakage flow until the mechanisms of blade tip stall finally dominate the aerodynamics.

For blade tip stall, the local mass flow near the blade tip has to be increased significantly by the casing treatment so that this mechanism is more loss-intensive in order to stabilize the compressor stage. This means, in the end, that the compressor efficiency is negatively influenced.

3. INVESTIGATED COMPRESSOR STAGE AND NUMERICAL MODEL

The investigated compressor stage is a transonic front stage of a modern high-pressure compressor (HPC). The compressor-rig totally consists of 4.5 stages. At design point, the total pressure ratio of the front stage including the IGV at the point of maximum efficiency is about 1.63. The compressor operates at a speed of 12 960 rpm and has a relative Mach number at the rotor 1 blade tip of about 1.3. The tip clearance of the rotor 1 is 0.5% span. Tip clearances of IGV and stator 1 were also modeled as a simplification of the gap resulting from the mechanism for the variable vanes.

The compressor-rig has been run in the past and is now numerically simulated in order to investigate different casing treatment geometries. After the selection of the most promising geometry, new experiments will be conducted in order to validate the results gained by the numerical simulations.

In order to save computational time and to be able to conduct unsteady simulations, the domain scaling approach was applied. The compressor stage was reduced to the blade numbers shown in Table 1.

Table 1: Simulated compressor blades.

Row	Original	Adapted	Simulated
IGV	40	46	2
Rotor 1	23	23	1
Stator 1	36	46	2

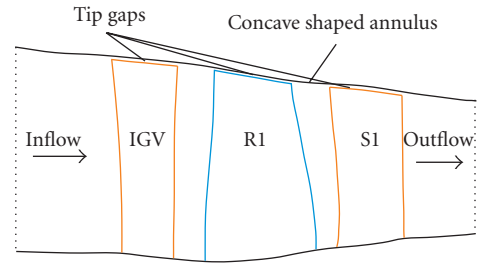

Figure 2: Simulated compressor stage.

The reduction in simulated passages for the discretization is based on the assumption that the flow is identical inside all blade passages of the rotor 1 and inside every 2nd blade passage of the IGV and stator 1, respectively. The IGV and stator 1 were not aerodynamically scaled due to the fact that the casing treatment is applied to the rotor and hence effects that destabilize the compressor have to appear at the rotor 1 tip and not at the IGV or stator 1, so that the difference in their aerodynamic loading due to the increased blade numbers is of no importance. The commercial solver NUMECA/EURANUS was used for the simulation. The integration in time is implemented through the implicit pseudo-time scheme. For the time-accurate investigations, 41 physical time steps per blade passage and 15 pseudo-time iterations with a CFL number of 1-2 within each physical time-step were simulated. The choice of a prim number for the number of time steps was made to dampen possible numerical oscillations excited by any blade periodicity. Turbulence is introduced with the one-equation turbulence model from Spalart-Allmaras. The simulations were conducted on 4 3.8 GHz Pentium IV processors with 2 GB RAM. Without an initial solution, about 4 weeks and several rotor rotations were required in order to achieve convergence. The numerical stall point was determined with an accuracy of 2500 Pa in static back pressure. Numerical stall appears as a transient flow field characterized by a continuous decrease in mass flow, total pressure, and efficiency. Numerical stall in the simulations was never a purely numerical phenomenon, but always arose from physical consequences due to distinctive flow mechanisms.

One blade passage is meshed with a block structured topology consisting of 4 H-blocks and 1 O-block around the blade. The H-blocks are located upstream of the leading edge, downstream of the trailing edge and, seen in circumferentially direction, in front and behind the blade O-grid. The whole grid for all meshed passages including 2 IGVs, one rotor and 2 stator passages, consists of 2.3 million mesh points without the mesh for the casing treatment. 77 grid

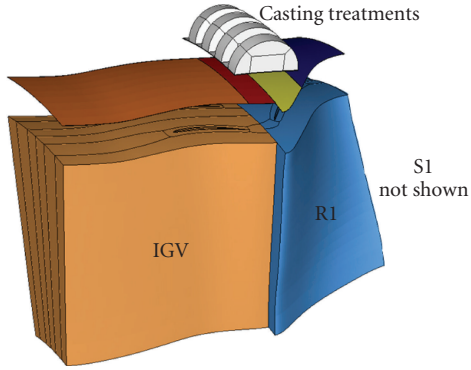

Figure 3: Block topology.

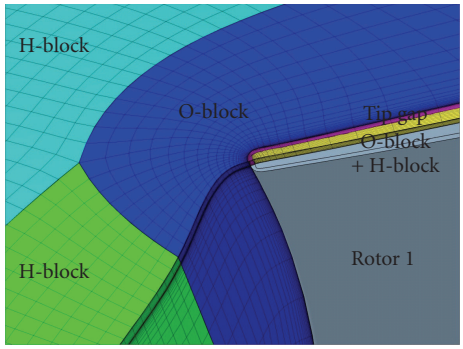

Figure 4: Mesh topology at Rotor 1 tip leading edge.

points were used to model the blade passage in the spanwise direction in all rows. For the blade-to-blade direction, in the rotor 59 grid points were used, whereas in the stators 29 per passage were used. In order to resolve phenomena occurring near the shroud, the radial distribution was refined in the direction toward the casing. The O-grid of Rotor 1 has 193 grid points in the circumferential direction to ensure a high-quality mesh at the leading and trailing edge of the rotor blade. The tip clearance is modeled by 21 grid points in radial direction. The tip gap is modeled with an H-Block in the middle and a surrounding O-Block. Because of the low-Reynolds description of the boundary layer in the Spalart-Allmaras model used to simulate the turbulence, the mesh was refined toward the solid boundaries in order to meet the resolution requirements of $y^+ \leq 2$. Mesh studies were conducted in steady simulations by coarsening and refining the mesh. This mesh size seemed to be the ideal compromise between accuracy and computational demands.

The casing treatments are resolved with about 100 000 grid points in a butterfly-mesh. The nonrotating grids of the casing treatments are mounted on a very thin circumferential socket (5% of the tip clearance) and linked to the moving rotor and fixed IGV passage by an unsteady rotor-stator interface using a sliding plane directly at the casing.

4. INVESTIGATED CASING TREATMENTS

The design and the position of the tested casing treatments is a well-known type. It has a significant impact on the stability on rotor flows as shown by several authors (e.g., Takata and Tsukuda [3]). The shape of the tested slots is a semicircle. This was done in order to improve flow circulation inside the casing treatment and to avoid unnecessary stagnation or secondary recirculation zones. No information is available about the ideal number of slots per passage: the slot height or slot width for a given compressor configuration in order to optimize both, efficiency and stability. The simulated casing treatments use the pressure gradient in the blade passage as well as the axial momentum of the main flow to create a flow circulation inside the slots. Additionally, the pressure gradient from the blade pressure to the blade suction side causes a secondary flow inside the casing treatment when the rotor passes underneath. The slots remove blockage fluid out of the blade passage and reinject the fluid further upstream near the IGV trailing edge. This type of casing treatment is often called self-recirculating casing treatment.

Main parameters of the casing treatment configurations can be seen in Figures 5 and 6. Due to spatial limitations, stator 1 is not shown in Figure 5. In configuration 1 and 2, the slots are parallel to the rotational axis, whereas in the inclined configurations 3 and 4, the slots have an angle of about 30° relative to the machine axis, so that they are parallel to the IGV's flow exit angle. Both configurations, the axial and the inclined one, were run with 4 equal slots per passage providing an open area of 50% in circumferential direction to the passage, and 2 equal slots per passage providing an open area of 25% to the passage. The axial extension of the slots is 80% of the axial rotor chord length. The axial position of the slots covers 30% of the blade chord length. The slots have a radial extension, thus are not inclined against a meridian plane in the direction of blade rotation.

5. FLOW MECHANISMS INSIDE THE IGV-ROTOR-STATOR CONFIGURATION WITHOUT CASING TREATMENT

Many authors have already described the mechanisms and characteristics of tip leakage flow and its resulting vortex in transonic compressor stages (Hofmann and Ballmann [17], Wilke and Kau [23]). Therefore, the description of the flow in the stage without the casing treatment will concentrate on the most important aspects in order to understand the occurring phenomena.

The tip leakage vortex develops because of the pressure difference between the pressure and suction side at the blade tip gap. The vortex core emerges near the leading edge of the blade, with a tendency to move more toward the blade leading edge when increasing static back pressure. Additionally the aerodynamic blade loading and thus the pressure difference at the blade tip increases when approaching stall, so that the tip leakage flow is also increased. This leakage flow rolls up around the vortex core coming from near the leading edge and forms the tip leakage vortex. This rotation of the tip leakage vortex results in the formation of a characteristic

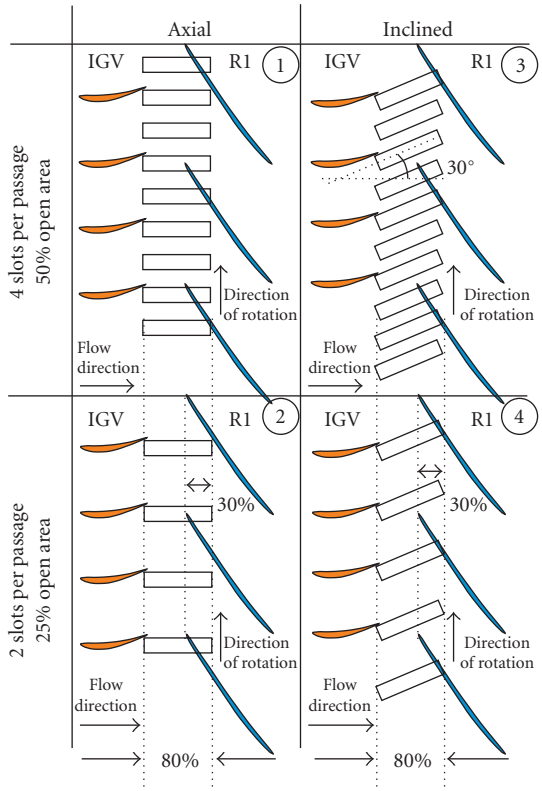

Figure 5: Simulated casing treatments.

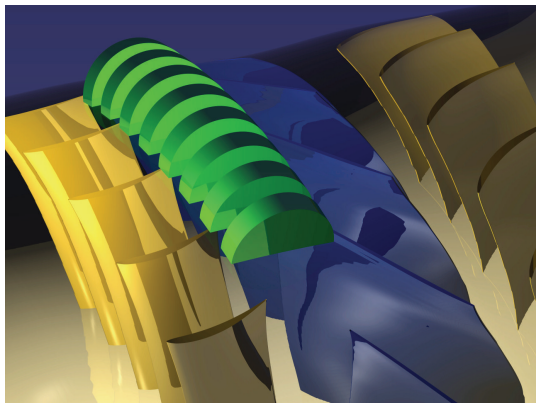

Figure 6: 3D view of casing treatment 1.

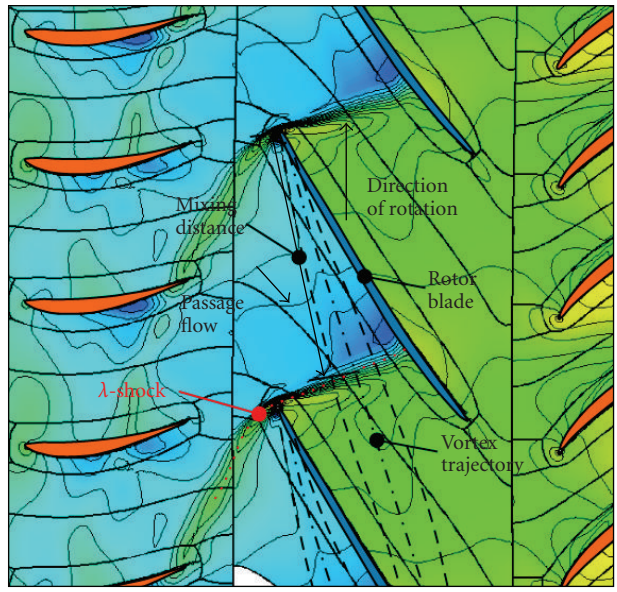

Figure 7: Static pressure in the blade passage at maximum efficiency, 98% blade height.

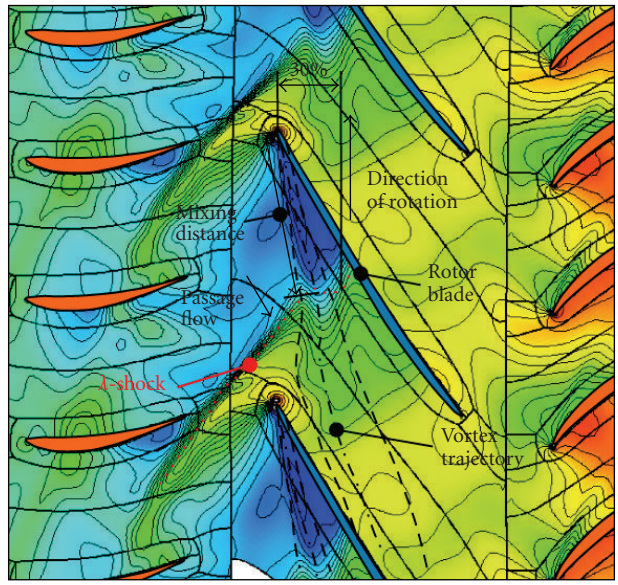

Figure 8: Static pressure in the blade passage at the onset of vortex breakdown, 98% blade height.

trough in the static pressure distribution (Figures 7 and 8). This trough indicates the vortex trajectory. Note that in the figures, only one time-step out of 41 is shown.

At maximum efficiency, the tip leakage vortex is able to cross the blade passage shock without being significantly disturbed (see Figure 7). Blockage effects are very small and can be neglected. The λ-Shock is attached to the leading edge of the blades and impinges on the suction side of the precursory blade at about 3/4 of the axial blade chord length. Hence, the low-energy tip leakage vortex emerging from the forward tip gap has enough time to be mixed and thus re-energized by the main passage flow. The trajectory of the vortex is straight, with a very small angle relative to the blade chord of the blade where it emerges, and it does not impinge on the pressure side of the following blade.

Near the onset of vortex breakdown, which is an operating point close to numerical stall (see Figure 8), the tip leakage vortex crosses the blade passage shock with a significant enlargement of the cross section of the vortex. Additionally, the trajectory turns into a direction more perpendicular to the blade main flow. This phenomenon is often called vortex breakdown. Blockage effects of the main flow are significant (Figures 8 and 9). The λ-Shock is detached from the blade leading edge and impinges on the suction

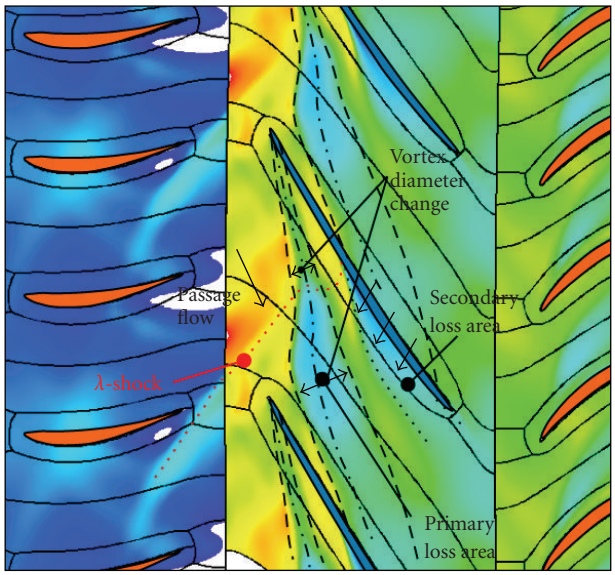

Figure 9: Relative total pressure at the onset of vortex breakdown, 98% blade height.

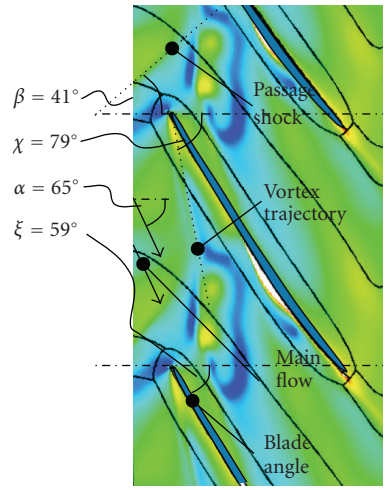

Figure 10: Flow angles at 99% blade height (flow angle: blue = 90°, red = 45°).

side of the precursory blade at about 1/2 of the axial blade chord length. Hence, the mixing distance for the low-energy tip leakage flow with the main flow is reduced to about 65% of the distance at the maximum efficiency operating point. As a consequence, the vortex does also not get the same level of re-energetization. Furthermore, the difference in static pressure before and after the shock is increased at operation points close to stall, marking an additional hurdle for the vortex to pass through. As a consequence, the vortex breaks up when passing the shock, increases its diameter, and changes direction. Additionally, what cannot be seen on the pictures, the inward radial extension increases significantly after the shock. In Figure 9, an additional loss mechanism at the operating point close to stall can be observed. As the vortex changes direction after the shock, it impinges onto the second half axial blade length on the pressure side of the following blade. This low-energy fluid passes the tip gap and creates a secondary loss area on the blade's suction side. The relative total pressure in Figure 9 illustrates these losses. The relative total pressure in front of the blade passage shock can even be lower than the static pressure right after the shock. This lack of energy blocks the core part of the leakage vortex from passing through the pressure barrier of the blade passage shock. As a consequence, the vortex core breaks down and the onset of a stagnation zone can be observed. Low-energy fluid, which cannot be transported through the shock, gets caught inside the stagnation zone. Under stable flow conditions, the fluid inside the stagnation zone gets re-energized continuously by mixing and diffusion processes between the core and outer parts of the vortex. This energy input prevents the breakdown area from continuous expansion. At surge, however, the re-energizing effects are no longer sufficient to dampen an expansion of the stagnation zone. Hence, more low-energy fluid is transported into the stagnation zone. The volume of the breakdown zone grows rapidly until the resulting blockage causes vast flow separations in the rotor flow. This mechanism finally leads to compressor stall.

6. CLASSIFICATION OF CRITICAL FLOW MECHANISMS

The classification of critical flow mechanisms in this compressor stage is determined based on the parameters defined by Wilke [24]. With these parameters, it can be decided whether the primary stall mechanism in the rotor is blade tip or tip blockage stall, as described in the second chapter. Several angles and the Mach number in front and after the shock near stall are required. For a detailed description, please refer to [24]. The Mach number in front of the passage shock is about 1.55, and after the shock about 0.8. To decide whether a blade tip stall is present, the factor B_P can be used.

This factor is defined in (1), the required flow angles close to stall can be found in Figure 10:

$$B_P = \frac{\alpha - \xi}{\chi - \xi} = 0.35. \quad (1)$$

For this compressor stage, this value is 0.35. In the case the value is 1, it is very likely that blade tip stall occurs, in case it is 0, it is very unlikely. Hence, for this stage, it is not very likely that blade tip stall occurs, which is a good condition for the application of axial slots. The second parameter to decide whether tip blockage stall is likely to occur is B_S:

$$B_S = \frac{M_{2,P,\text{crit}}}{M_{2,P}} = 0.772. \quad (2)$$

The critical Mach number $M_{2,P,\text{crit}}$ can be determined according to the following equation:

$$M_{2,P,\text{crit}} = M_1 \tan(90^\circ - \beta) \cos(180^\circ - (\alpha + \beta)). \quad (3)$$

In case the value for B_S equals 1, it is very likely that tip blockage stall occurs. This compressor stage has a value of

0.772, so that it is very likely that this type of stall is present in this rotor. As a consequence, this rotor seems to be an ideal candidate for the application of axial slots to enhance the stall margin.

7. FLOW MECHANISMS INSIDE THE IGV-ROTOR-STATOR CONFIGURATION WITH CASING TREATMENTS

Due to the time requirements of the calculations, only for the most promising—smallest loss of efficiency—configurations, the complete compressor lines were calculated. The configurations 2 and 4 with only 2 treatments per passage showed the smallest loss of efficiency. In the following figure, the passage flow is analyzed on the basis of configuration 2 and at one time step out of 41. In Figure 11, the static pressure distribution at 98% blade height with the casing treatment configuration 2 is shown. By comparing to Figure 7, which is at about the same mass flow level, it can be observed that the shock has moved a bit downstream, thus increasing the mixing distance of the vortex with the main flow. Additionally, the vortex trajectory has moved more toward the blade suction side from where it emerges. In the sketched slot outline, the mass flow density in the casing treatments is plotted. In this operation point, it can be seen that fluid enters as expected on the pressure side of the blade (red colored) and exits the slots (blue colored) upstream near the trailing edge of the IGVs. The main driving force for the slot circulation is the high-pressure zone in front of the blade's pressure side and after the shock. It takes place every time, when the blade leading edge passes the slot. The slot flow has a highly unsteady character. It is described in detail in the next chapter. For a point near stall, the observations as described above are similar. Important to note is that the characteristic low static pressure trough of the vortex between the leading edge and in front of the shock is reduced. That means that a higher static pressure occurs in the situation with the casing treatment at the same mass flow levels (not shown).

8. FLOW MECHANISMS INSIDE THE CASING TREATMENTS

Figure 12 illustrates the flow mechanisms in the casing treatments for configuration 1 with 4 slots per passage, in order to be able to describe the difference of the location of the slots near the IGV suction side trailing edge or in between two IGVs. The pictures illustrate the situation at a static back pressure of 140 kPa, still with a certain margin from stall. Only the most important phases of a period are shown. These are time steps 1 and 8, as well as time steps 21 and 28. The pictures on the left show the static pressure distribution in a plane located in the middle of the regarded casing treatment as well as the static pressure distribution in 98% blade height at time steps 1, 8, 21, and 28 of 41. The right sketches explain the occurring primary and secondary flow phenomena in the slots of CT1. Due to mass inertia effects, the pressure-induced flow mechanisms in the slots appear with a delay, so that the pressure patterns

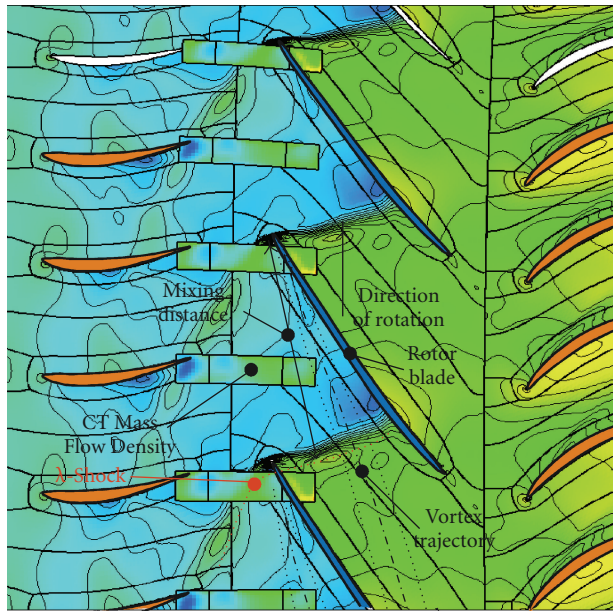

Figure 11: Static pressure in the blade passage with CT at maximum efficiency, 98% blade height.

in time step 1 (and 21) (left picture) show their effect on the flow only in step 8 (or 28, resp.) (see right sketch). Effects from the blade, here the vortex and the shock, show immediate impact on the flow and are here secondary flow effects.

8.1. Time step 1

In time step 1, a typical flow for axial slots is present. The flow enters the casing treatment on the right side, forming the main slot vortex, which is leaving the treatment upstream of the main flow near the IGV. The flow is mainly pressure driven, induced by a high-pressure field, which enters the slot directly after the shock. This is the primary cause for the development of the vortex in this time step. Secondary flow effects appear due to the shock itself. The main flow develops radially inwards in front of the shock, and is oriented radial outwards directly after the shock. The pressure pattern inside the slot shows a high pressure on the right side, resulting from the shock, and a low pressure on the left side.

8.2. Time step 8

In time step 8, this pressure pattern of time step 1 shows its effect, so that the main flow direction is from the right to the left, without any vortex. This main flow direction is supported by an additional impulse resulting from the blade tip that just passes the opening of the slot. Secondary flow effects result again from the shock itself, and from the tip gap vortex, producing a low-pressure field with an anticlockwise circulation. This extended vortex area also picks up some fluid, so that a small secondary flow appears above the vortex.

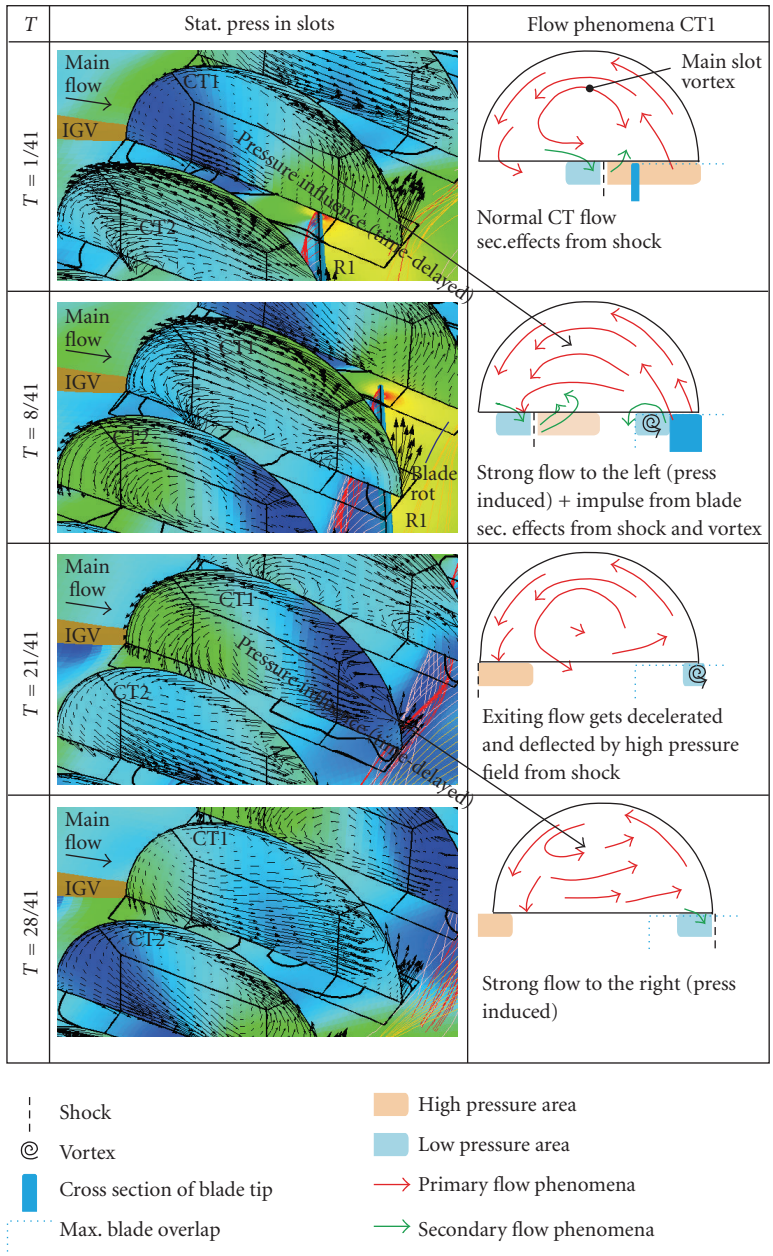

Figure 12: Casing treatment flow phenomena.

8.3. *Time step 21*

In time step 21, the high-pressure field from the shock which moved from the right to the left reaches the exit area of the main flow. However, the high-pressure field from right behind the blade passage shock also just passes underneath that area, so that the exiting flow gets decelerated and deflected. In this phase, the general flow inside the slot again looks like a typical casing treatment flow with a main slot vortex. In contrast to time step 1, the pressure pattern is reversed. The high-pressure field is on the left side, resulting from the shock, and the low-pressure field is on the right side, resulting from the low static pressure trough caused by the tip gap vortex. This pressure pattern has a strong influence on the flow phenomena in the next time step.

8.4. *Time step 28*

In this time step, the flow follows, again time-delayed, the pressure gradient and hence flows mainly from the left to the right, with only a small portion of the flow running in the "normal" anticlockwise direction near the outer part of the slot.

9. DIFFERENCE OF FLOW MECHANISMS IN CASING TREATMENT 1 AND 2

The main reason why configuration 1 is shown in Figure 12 is to illustrate the differences in the flow of casing treatment 1, located right at the suction side of the trailing edge of the IGV, and casing treatment 2, located in the middle of

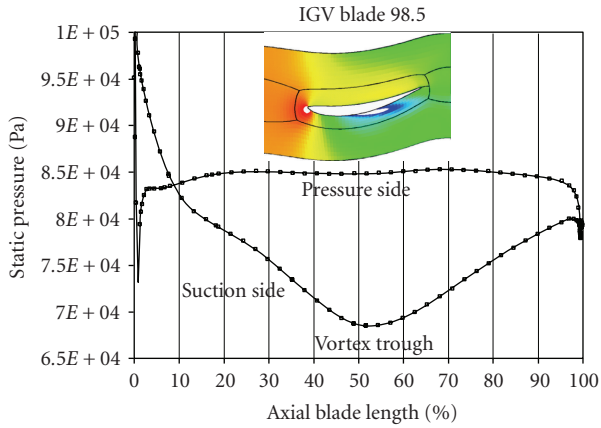

Figure 13: Static pressure around IGV at smooth wall, time averaged, 98% blade height.

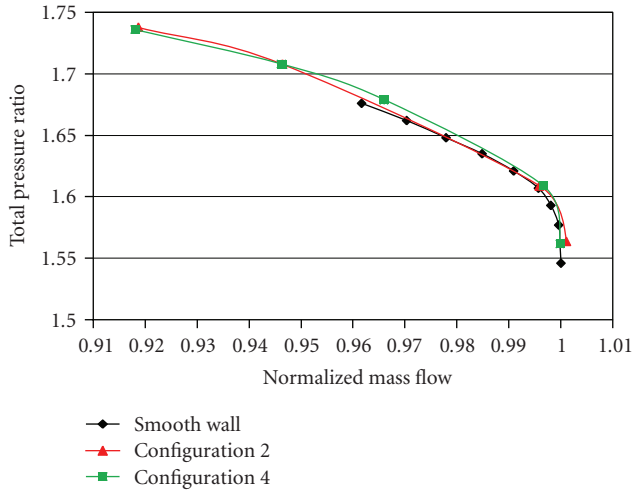

Figure 14: Total pressure ratio for smooth wall configuration and casing treatment configurations 2 and 4.

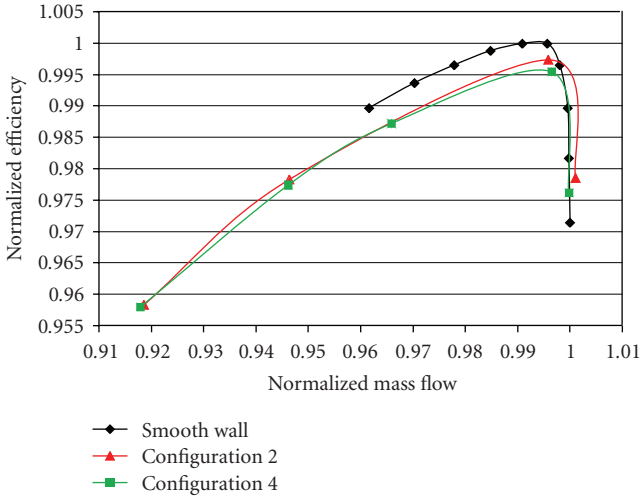

Figure 15: Normalized efficiency for smooth wall configuration and casing treatment configurations 2 and 4.

the two IGVs. The basic flow phenomena are the same, however there is one important difference as a result from the interaction of the shock and the IGVs suction and pressure side. In Figure 13, the time-averaged static pressure distribution around the IGV for the smooth wall case at 98% blade height is plotted. The high-pressure area behind the shock interacts with the IGV and its pressure distribution. As the pressure difference near the IGV trailing edge is about 100 000 Pa from the pressure to the suction side, the resulting local pressure from the interaction of the shock induced high-pressure field and the pressure distribution from the IGV is also different. The local bubble at the suction side has a lower static pressure than on the pressure side, consequently the deceleration and deflection of the flow as described for time steps 21 and 28 are weaker in this slot (CT1) than in the slot located between the IGVs (CT2).

10. COMPRESSOR STAGE MAPS

Figures 14 and 15 show the total pressure ratio and the normalized efficiency for the configurations 2 and 4 with casing treatments. For both configurations, a slight enhancement in total pressure ratio could be achieved at the same mass flow levels. However, the efficiency of configuration 2 is negatively influenced and is reduced by about 0.26% in comparison to the smooth wall configuration. For the configuration 4, the efficiency was even decreased by about 0.45%.

In order to evaluate the improvement in stall margin, the following equation is used for the determination:

$$\Delta SM_{CT} = \frac{\Pi_{\max,CT}}{\Pi_{\max,SW}} \frac{\dot{m}_{\min,SW}}{\dot{m}_{\min,CT}} - 1. \tag{4}$$

According to (4), the stall margin for both casing treatment configurations could be improved by about 8.6%.

11. CONCLUSION

This article has presented a numerical investigation on axial slots for a transonic axial compressor stage including IGV. Therefore, the stage was investigated with the methodology of Wilke. Tip blockage stall was identified as the primary stall mechanism in the rotor, so that the rotor is an ideal candidate for the application of axial slots for enhancing the stall margin. Four different casing treatment configurations were tested. The flow in the casing treatments has been analyzed in detail, with special focus on the interaction of the casing treatment flow and the influence of the IGV. At operating points on the right side of the compressor line, when the compressor is dethrottled, the flow phenomena in the slots are very similar, almost independent from the location of the slots relative to the IGV. At operating points close to surge on the left side of the compressor line, there is a significant difference in the flow phenomena inside the slots due to the interaction of the shock with the pressure distribution of the IGV. The typical slot vortex is more stable over time in the slots near the suction side leading edge of the IGV than in the slots between the IGVs. All casing treatment configurations decreased the overall stage efficiency, but they were also able to shift the stall margin by almost 9%. In future

investigations, one special focus will be put on the shape of the casing treatment in order to reduce the efficiency losses. Furthermore, the IGV will be closed for part speed. It can be expected that effects described in this article will get even stronger in that case.

NOMENCLATURE

HPC: High-pressure compressor
α: Main flow angle
β: Passage shock angle
γ: Relative angle mainflow—passage shock
χ: Vortex trajectory angle
ξ: Stagger angle
M_1: Mach-number in front of the shock
$M_{2,P}$: Perpendicular component of Mach-number after the shock
$M_{2,P,\text{crit}}$: Critical perpendicular component of Mach-number after the shock.

ACKNOWLEDGMENTS

the investigations presented in this article were conducted within the German collaboration program "AG Turbo-COOREFF" under Contract no. 0327710G and were funded by the Bundesministerium für Wirtschaft und Technologie (BMWi) and Rolls-Royce Deutschland Ltd. & Co. KG.

REFERENCES

[1] R. D. Moore, G. Kovich, and R. J. Blade, "Effect of casing treatment on overall and blade-element performance of a compressor rotor," NASA TN D-6538, 1971.

[2] D. C. Prince, D. C. Wisler, and D. E. Hilvers, "Study of casing treatment stall margin improvement," NASA CR-134552, 1974.

[3] H. Takata and Y. Tsukuda, "Stall margin improvement by casing treatment—its mechanism and effectiveness," *ASME Journal of Engineering for Power*, vol. 99, no. 1, pp. 121–133, 1977.

[4] E. M. Greitzer, J. P. Nikkanen, D. E. Haddad, R. S. Mazzawy, and H. D. Joslyn, "A fundamental criterion for the application of rotor casing treatment," *ASME Journal of Fluids Engineering*, vol. 101, no. 2, pp. 237–243, 1979.

[5] J. Paulon and D. Dehondt, "Influence of casing treatment on the operating range of axial compressors," ASME Paper 82-GT-103, 1982.

[6] G. D. J. Smith and N. A. Cumpsty, "Flow phenomena in compressor casing treatment," *Journal of Engineering for Gas Turbines and Power*, vol. 106, no. 3, pp. 532–541, 1984.

[7] A. R. Azimian, R. L. Elder, and A. B. McKenzie, "Application of recess vaned casing treatment to axial flow fans," ASME Paper 89-GT-68, 1989.

[8] D. W. Thompson, P. I. King, and D. C. Rabe, "Experimental investigation of stepped tip gap effects on the performance of a transonic axial-flow compressor rotor," ASME Paper 97-GT-7, 1997.

[9] M. D. Hathaway, "Self-recirculating casing treatment concept for enhanced compressor performance," NASA TM-2002-211569, 2002.

[10] D. C. Rabe and C. Hah, "Application of casing circumferential grooves for improved stall margin in a transonic axial compressor," ASME Paper GT-2002-30641, 2002.

[11] I. Wilke and H.-P. Kau, "A numerical investigation of the flow mechanisms in a HPC front stage with axial slots," ASME Paper GT-2003-38481, 2003.

[12] I. Wilke, H.-P. Kau, and G. Brignole, "Numerically aided design of a high-efficient casing treatment for a transonic compressor," ASME Paper GT2005-68993, 2005.

[13] G. Brignole, H.-P. Kau, and I. Wilke, "Numerical evaluation of important parameters ruling the effectiveness of casing treatments in transonic compressors," ISABE Paper ISABE-2005-1095, 2005.

[14] X. Lu, W. Chu, J. Zhu, and Y. Wu, "Mechanism of the interaction between casing treatment and tip leakage flow in a subsonic axial compressor," ASME Paper GT2006-90077, 2006.

[15] X. Lu, W. Chu, J. Zhu, and Y. Wu, "Experimental and numerical investigation of a subsonic compressor with bend skewed slot casing treatment," ASME Paper GT2006-90026, 2006.

[16] M. W. Müler, H.-P. Schiffer, and C. Hah, "Effect of circumferential grooves on the aerodynamic performance of an axial single-stage transonic compressor," ASME Paper GT2007-27365, 2007.

[17] W. Hofmann and J. Ballmann, "Tip clearance vortex development and shock-vortex-interaction in a transonic axial compressor rotor," AIAA Paper 2002-0083, 2002.

[18] W. Hofmann and J. Ballmann, "Some aspects of tip vortex behavior in a transonic turbocompressor," ISABE Paper ISABE-2003-1223, 2003.

[19] S. Schlechtriem and M. Lötzerich, "Breakdown of tip leakage vortices in compressors at flow conditions close to stall," ASME Paper 97-GT-041, 1997.

[20] M. Furukawa, M. Inoue, K. Saiki, and K. Yamada, "The role of tip leakage vortex breakdown in compressor rotor aerodynamics," ASME Paper 98-GT-239, 1998.

[21] M. Hoeger, G. Fritsch, and D. Bauer, "Numerical simulation of the shock-tip leakage vortex interaction in a HPC front stage," ASME Paper 98-GT-261, 1998.

[22] I. Wilke and H.-P. Kau, "A numerical investigation of the flow mechanisms in a high pressure compressor front stage with axial slots," *Journal of Turbomachinery*, vol. 126, no. 3, pp. 339–349, 2004.

[23] I. Wilke and H.-P. Kau, "A numerical investigation of the influence of casing treatments on the tip leakage flow in a HPC front stage," ASME-Paper GT-2002-20642, 2002.

[24] I. Wilke, *Verdichterstabilisierung mit passive Gehäusestrukturierungen—eine numerische Analyse*, Ph.D. dissertation, Institute of Flight Propulsion, Technische Universität München, Munich, Germany, 2005.